Journal of Hazardous Materials 160 (2008) 173–180

Contents lists available at ScienceDirect

Journal of Hazardous Materials

journal homepage: www.elsevier.com/locate/jhazmat

Adsorption properties of Congo Red from aqueous solution onto surfactant-modified montmorillonite

Li Wang[a,b], Aiqin Wang[a,*]

[a] Center of Eco-material and Green Chemistry, Lanzhou Institute of Chemical Physics, Chinese Academy of Sciences, Lanzhou 730000, PR China
[b] Graduate School of the Chinese Academy of Sciences, Beijing 100049, PR China

ARTICLE INFO

Article history:
Received 12 May 2007
Received in revised form 19 January 2008
Accepted 27 February 2008
Available online 4 March 2008

Keywords:
Montmorillonite
Surfactant
Adsorption
Congo Red
Kinetic

ABSTRACT

A series of surfactant-modified montmorillonites (MMT) were prepared using octyltrimethylammonium bromide (OTAB), dodecyltrimethylammonium bromide (DTAB), cetyltrimethylammonium bromide (CTAB) and stearyltrimethylammonium bromide (STAB), and the organification of MMT was proved by Fourier transform infrared (FTIR) spectroscopy, X-ray diffraction (XRD), scanning electron micrographic (SEM) and transmission electron microscope (TEM). The adsorption of Congo Red (CR) anionic dye from aqueous solution onto surfactant-modified MMT was carried out. Compared with MMT, the adsorption capacity of surfactant-modified MMT for CR was greatly enhanced and MMT modified with CTAB (2.0 CEC) exhibited the higher adsorption capacity. The effects of pH value of the dye solution, adsorption temperature, adsorption time and the initial dye concentration on the adsorption capacity of CR on CTAB-MMT have been investigated. The results showed that the adsorption kinetic of CR on CTAB-MMT could be best described by the pseudo-second-order model and that the adsorption isotherm of CR was in good agreement with the Langmuir equation. The IR spectra and SEM analysis also revealed that the adsorption of CTAB-MMT was a chemical adsorption process between CTAB and the NH_2, –N=N– and SO_3 groups of CR.

1. Introduction

Many industries generate coloured effluents containing various dyes and pigments and discharge the same to natural water bodies [1]. Among these dyes and pigments, many are toxic and have carcinogenic and mutagenic effects that affect aquatic biota and also humans [2–4]. So, coloured effluents have to be adequately treated before they are discharged into the environment.

Dyes are generally difficult to be biodegradated and photodegradated, therefore, there are several problems in the treatment of dyes from industrial wastewater. Many different treatment techniques including biological treatment, coagulation, floatation, oxidation, ozonation and nanofiltration have been used in the removal of colored dyes from wastewater [5–7]. However, adsorption is one of the effective methods with the advantages of high treatment efficiency and no harmful by-product to treated water [8].

There are a lot of non-conventional, low cost adsorbents such as biogas waste slurry [9], waste banana pith [10], paddy straw [11], waste Fe(III)/Cr(III) hydroxide [12], waste orange peel [13], waste red mud [14], calcium-rich fly ash [15] and so on have been used for Congo Red (CR) dye removal. But the adsorption capacity of these adsorbents is not large. Activated carbon has been the most widely used adsorbent because of its high capacity for the adsorption of coloured dyes [16]. However, adsorbent-grade activated carbon is cost-prohibitive and both regeneration and disposal of the used carbon are often very difficult. Recently, clay materials are being widely considered as alternative low cost adsorbents owing to they can be easily obtained and regenerated.

Among many kinds of clay minerals, montmorillonite (MMT) clays have often been used in the remove of organic pigments and dyes [17–21] due to their high surface area and high cation exchange capacity. However, MMT adsorb the anionic dyes only onto the external broken-bonds surface in very small amounts. Therefore, in order to improve their adsorption capacities for anionic dyes, the surface of MMT was modified by a suitable approach. There are many exchangeable cations on the surface of MMT, the cationic surfactants are generally used as modifiers. The characteristics of these so-called organoclays can be changed by variation of surfactant properties [22], such as alkyl chain length [23,24], number and branches [25,26]. The surface properties of the clays modified by surfactants altered from organophobic to organophilic, which aids in improving clay adsorption for organic compounds [23,27]. In recent 20 years, many reports [28–31] showed that the surfactant-modified clays displayed

* Corresponding author. Tel.: +86 931 4968118; fax: +86 931 8277088.
E-mail address: aqwang@lzb.ac.cn (A. Wang).

0304-3894/$ – see front matter © 2008 Elsevier B.V. All rights reserved.
doi:10.1016/j.jhazmat.2008.02.104

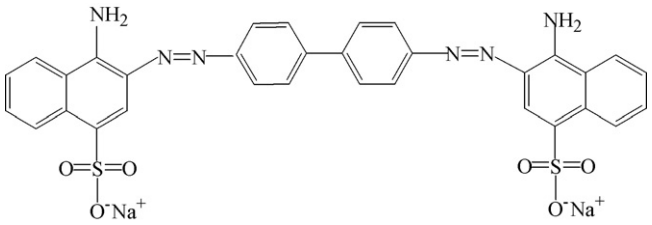

Fig. 1. Structure of CR (molecular formula: $C_{32}H_{22}N_6O_6S_2Na_2$).

higher adsorption capacity than the original clay. Although the modification of clays with surfactants increases their cost significantly, the resultant increase in adsorption capacity may still make surfactant-modified clays cost effective. So clay derivatives may be promising sorbents for environmental and purification purposes.

So far, the study on CR dye adsorption using surfactant-modified MMT has not been reported in literature. Therefore, a series of surfactant-modified MMT were prepared using octyltrimethylammonium bromide (OTAB), dodecyltrimethylammonium bromide (DTAB), cetyltrimethylammonium bromide (CTAB) and stearyltrimethylammonium bromide (STAB), and the effects of pH value of the dye solution, adsorption temperature, adsorption time and the initial dye concentration on the adsorption capacity of CR on CTAB-MMT have been investigated. The adsorption kinetics and isotherms for CR dye onto CTAB-MMT were also studied, and the mechanism of CR adsorption was discussed.

2. Experimental

2.1. Materials

Natural MMT are procured from Shandong Longfeng Montmorillonite Co., China. Purified MMT was obtained as follows: 6.0 g of natural MMT was dispersed in 300 mL distilled water. After stirring for 1 h at 6000 rpm with a mechanical stirrer, then the clay suspension was left to stand overnight at 250 rpm at room temperature. The slurry was centrifuged at 1500 rpm for 5 min and the suspension was transferred to a tank that was continuously centrifuged at 4500 rpm for 30 min. After eliminating the supernatant, the solid was dried in an air oven at 105 °C for 4 h, ground and sieved to 200 mesh size to obtain purified MMT. The cationic exchange capacity (CEC) of the sample is 102.8 mequiv/100 g. Chemical analysis of purified MMT was performed by the PANalytical Company with a Magix PW 2403 XRF Spectrometer and the results are shown in Table 1. The molecular weight of CR (Tianjin Kermel Chemical Reagent Co., China) is 696.66 g/mol. The molecular structure of CR is shown in Fig. 1. OTAB, DTAB, CTAB and STAB were obtained from Alfa Aesar Tianjin Chemical Reagent Co., China. Other agents used were analytical grade and all solutions were prepared with distilled water.

2.2. Preparation of surfactants-modified MMT

The synthesis of surfactant-modified MMT was conducted by the following procedure. Each surfactant (OTAB, DTAB, CTAB and STAB) containing the amount of surfactant equivalent to 1.0 of the CEC of purified MMT was firstly dissolved in 100 mL distilled water and then 4.0 g purified MMT was slowly added. The reaction mixtures were stirred continuously at room temperature for 12 h. The mixture was filtered and washed several times with distilled water until no bromide ion was detected by $AgNO_3$ solution (0.1 M). The surfactant-modified MMT was dried in an air oven at 105 °C for 4 h and ground to 200 mesh size.

The preparation procedure of a series of CTAB-MMT is similar to that of preparation of surfactants-modified MMT except that CTAB with 0.25, 0.5, 0.75, 1.0, 1.5, 2.0, 2.5 and 3.0 CEC of MMT were added to the reaction system.

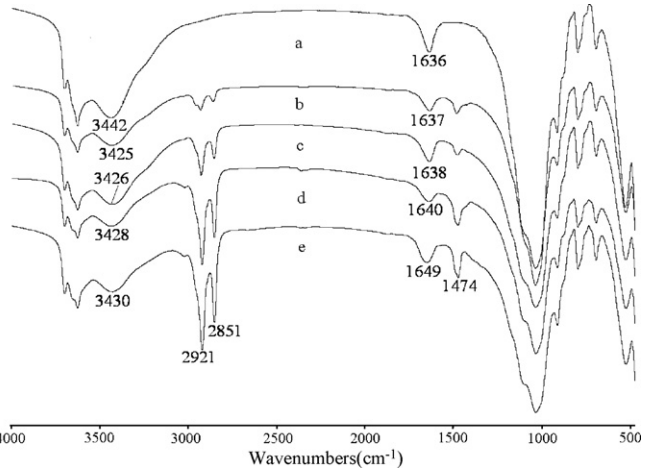

Fig. 2. IR spectra of purified MMT (a), OTAB-MMT (b), DTAB-MMT (c), CTAB-MMT (d) and STAB-MMT (e).

2.3. Adsorption experiments

The batch adsorption was carried out on a thermostated shaker (THZ-98A) operated at 120 rpm. In the test for investigation of the effect of different kinds of surfactant and different amounts of CTAB on adsorption capacities of CR experiments, 0.05 g adsorbent and 25 mL CR solution (initial concentration 800 mg/L, natural pH 7.5) were used. The system was maintained under shaking at 30 °C until adsorption equilibrium was reached. The influence of pH on CR removal was studied by adjusting CR solutions (1000 mg/L) to different pH values (DELTA-320, 4.0, 5.0, 6.0, 7.0, 8.0 and 9.0) using 0.1 mol/L HCl or NaOH solution and agitating 25 mL dye solution with 0.05 g adsorbent at 30 °C for 480 min. The effect of temperature on dye removal was carried out in the 25 mL dye solutions (1000 mg/L, pH 7.0) by adding 0.05 g adsorbent until equilibrium was achieved. The effect of adsorption time on dye removal was carried out in the 25 mL dye solutions (1000 mg/L, pH 7.0) by adding 0.05 g adsorbent at 30 °C for predetermined intervals of time. The effect of the initial dye concentration on dye removal were carried out by agitating 25 mL various dye concentrations of CR solution at pH 7.0 by adding 0.05 g adsorbent at 30 °C for 480 min.

After adsorption was over, the mixture was rapidly centrifuged in a laboratory centrifuge at 4500 rpm for 10 min. The concentration

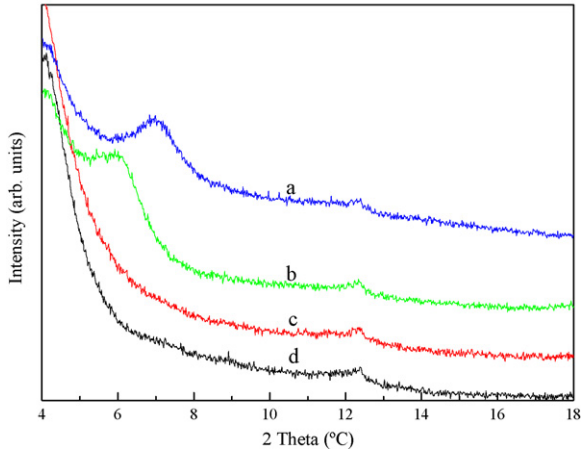

Fig. 3. XRD powder patterns of purified MMT (a), CTAB-MMT with CTAB of 0.5 (b), 1.0 (c) and 2.0 (d) CEC of MMT.

Table 1
Chemical composition of purified MMT

Component	SiO_2	Al_2O_3	Fe_2O_3	Na_2O	MgO	CaO	TiO_2	K_2O	SO_3	P_2O_5	MnO
Weight (%)	61.92	20.84	9.36	2.60	1.65	1.55	1.21	0.50	0.10	0.08	0.02

of dye was determined using a Specord 200 UV/vis spectrophotometer. The absorbance at a specific wavelength was measured for CR (500 nm). A calibration curve for CR was constructed by diluting the solution to various known concentrations and recording their absorbance at 500 nm. The adsorption capacity of CR was calculated through the following equation:

$$q_e = \frac{(C_0 - C_e)V}{m} \quad (1)$$

where q_e is the amount of adsorption dye (mg/g) at equilibrium, C_0 is the initial concentration of CR in solution (mg/L), C_e is the equilibrium concentration of CR in solution (mg/L), m is the mass of adsorbent used (g) and V is the volume of CR solution (L). In the method of calculating q_e, no losses of CR to any other mechanism (volatilization, sorption to the glassware, degradation, etc.) were assumed.

2.4. Characterization

IR spectra of the samples were characterized using a FTIR Spectrophotometer (Thermo Nicolet, NEXUS, TM) in KBr pellets. XRD analyses of the powdered samples were performed using an X-ray power diffractometer with Cu anode (PAN Alytical Co. X'pert PRO), running at 40 kV and 30 mA, scanning from 4° to 18° at 3° min^{-1}. The surface area and average pore size of the samples were measured using an Accelerated Surface Area and Porosimetry System (Micromeritics, ASAP 2010) by BET-method at 76 K. Micrographs of the samples were taken using an SEM (JSM-6701F, JEOL, Ltd.). Before observation of SEM, all samples were fixed on aluminum stubs and coated with gold. TEM images analysis of the samples were examined on a TEM (JEM 1200-EX) at 75–100 kV.

3. Results and discussion

3.1. FTIR analysis of surfactants-modified MMT

The infrared spectra of purified MMT (a), OTAB-MMT (b), DTAB-MMT (c), CTAB-MMT (d) and STAB-MMT (e) are shown in Fig. 2. Compared with the IR spectra of purified MMT, the absorption band at 3442 cm^{-1}, corresponding to –OH stretching vibration of H_2O of MMT, weakened and shifted to the lower wave number 3425 cm^{-1}

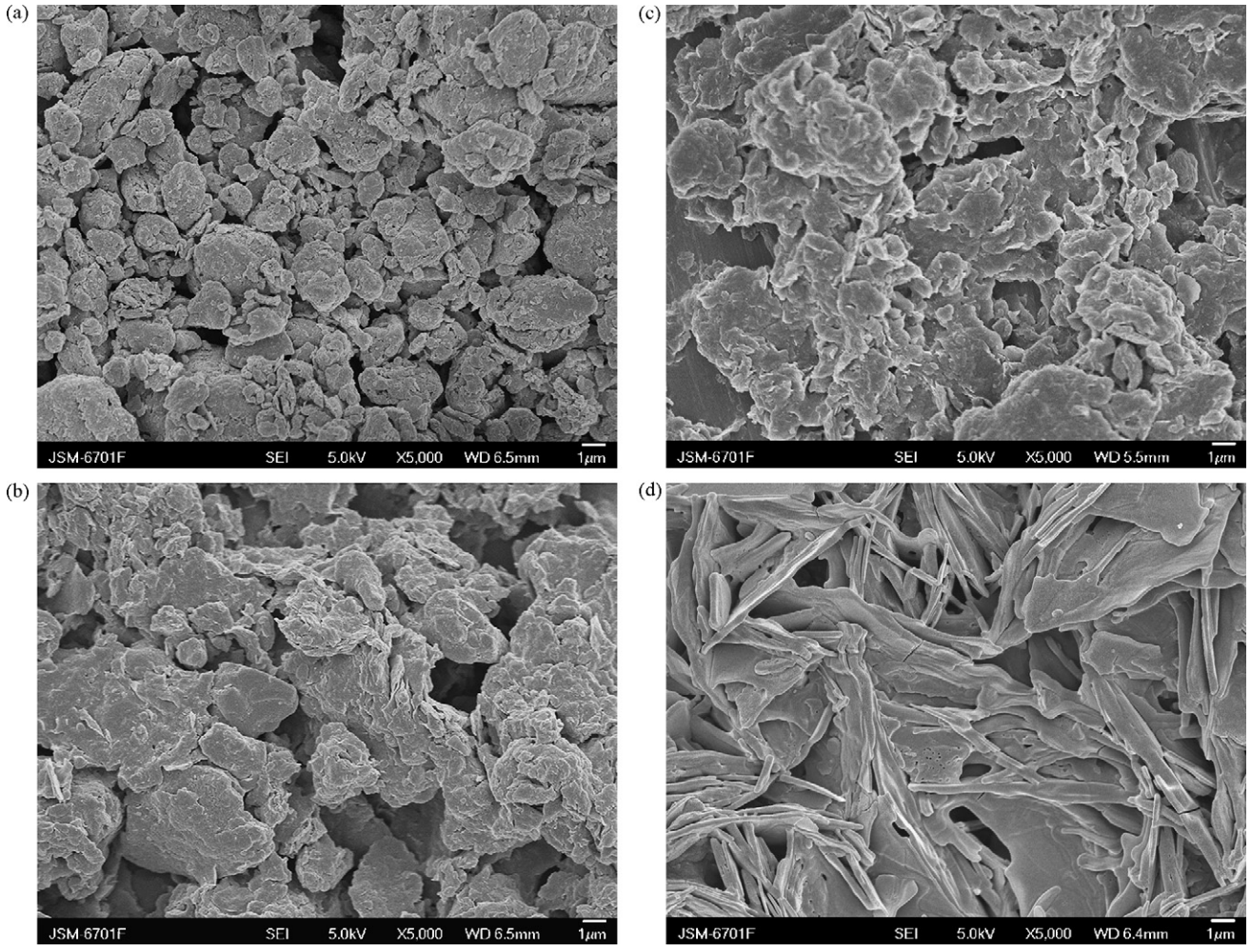

Fig. 4. SEM images of purified MMT (a), CTAB-MMT with CTAB of 0.5 (b), 1.0 (c) and 2.0 (d) CEC of MMT.

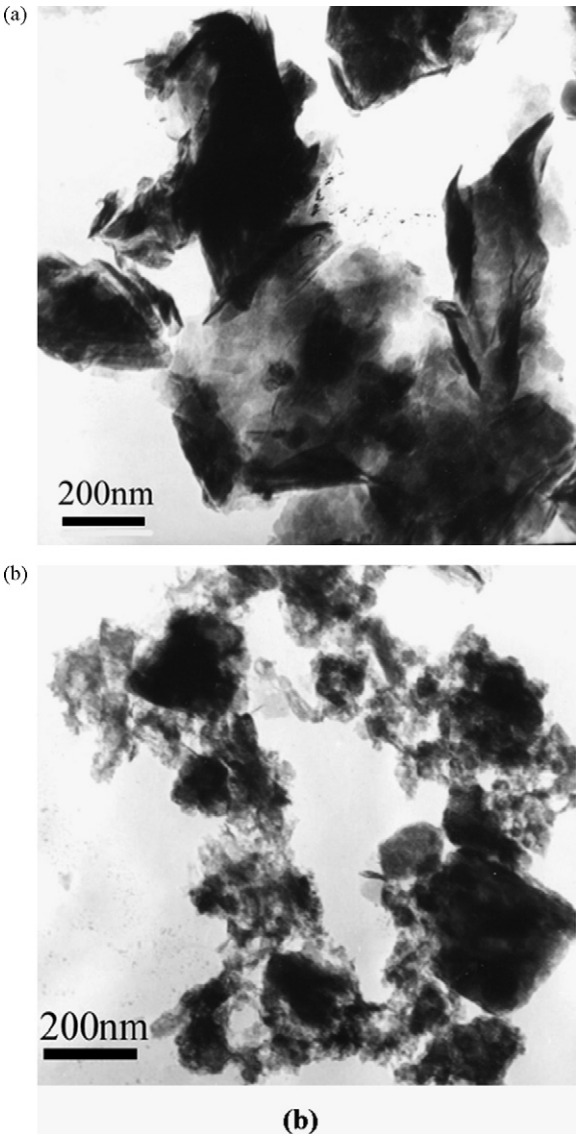

Fig. 5. TEM images of purified MMT (a) and CTAB-MMT with CTAB of 2.0 (b) CEC of MMT.

(Fig. 2b), 3426 cm^{-1} (Fig. 2c), 3428 cm^{-1} (Fig. 2d) and 3430 cm^{-1} (Fig. 2e). In addition, the characteristic absorption bands of the symmetric and asymmetric stretching vibrations of the $-CH_2$ (2851 cm^{-1}) and $-CH_3$ (2921 cm^{-1}), and the bending vibrations of $-CH_3$ (1474 cm^{-1}) were observed on the IR spectra of surfactant-modified MMT. Moreover, the intensity of these bands increases with the increase of the number of carbon atoms of surfactants. This indicated that the interaction reaction between MMT and surfactant molecules had taken place during the modifying process. Compared with the IR spectra of purified MMT, the absorption band of –OH bending vibration of H_2O of MMT (1636 cm^{-1}) moved to 1637 (Fig. 2b), 1638 (Fig. 2c), 1640 (Fig. 2d) and 1649 cm^{-1} (Fig. 2e). Simultaneously, the intensity of this absorption band decreases, which indicated the H_2O content reduced with the replacement of the hydrated cations by surfactant cation ions. This observation showed that the surface properties of MMT had been changed from hydrophilic to hydrophobic by modifying it with surfactants. The Infrared spectra of the CTAB-MMT with the different quantities of CTAB are similar to those of surfactants-modified MMT.

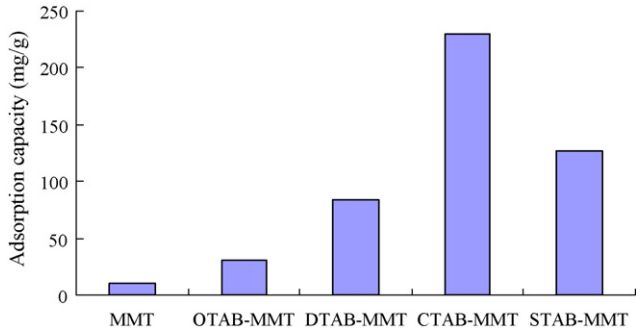

Fig. 6. Effect of the surfactants (1.0 CEC used for each of the different surfactant types) on adsorption capacity of surfactant-modified MMT for CR. Adsorption experiments—dye concentration, 800 mg/L; sample dose, 0.05 g/25 mL; natural pH 7.5; temperature, 30 °C; equilibrium time, 480 min.

3.2. XRD analysis of CTAB-MMT

Fig. 3 illustrates the XRD patterns of purified MMT (Fig. 3a) and CTAB-MMT with different quantities of CTAB, equal to 0.5 (b), 1.0 (c), 2.0 (d) CEC of MMT. A typical diffraction peak of purified MMT (Fig. 3a) is 6.94°, responding to a basal spacing of 12.74 Å. After intercalation with CTAB, this peak disappears. The movement of the typical diffraction peak of MMT to lower angle (5.94°), responding to a basal spacing of 14.89 Å (Fig. 3b), which indicates the formation of the intercalated nanostructure with the amount of CTAB of 0.5 CEC of MMT. The intensity of the peak disappears with further increasing of the amount of CTAB indicated that the formation of the exfoliated nanostructure in CTAB-MMT.

3.3. SEM image analysis of CTAB-MMT

The morphologies of purified MMT (a), CTAB-MMT with CTAB of 0.5 (b), 1.0 (c), 2.0 (d) CEC of MMT are shown in Fig. 4. It can be seen from this figure that purified MMT shows a small particles and non-porous surface (Fig. 4a), but the introduction of CTAB lead to a large particles and coarse porous surface. Moreover, this phenomenon becomes obvious with an increase of CTAB. The incorporation of CTAB can form large particles and numerous cavities, which may be convenient for the penetration of dye molecules into the galleries of CTAB-MMT and result in an increase in the absorption capacity of CR on CTAB-MMT.

3.4. TEM image analysis of CTAB-MMT

Fig. 5 shows the TEM images of purified MMT (a) and CTAB-MMT with CTAB of 2.0 (b) CEC of MMT. As shown in Fig. 5, compared with MMT (Fig. 5a), stacks of multilayers of CTAB-MMT (Fig. 5b) became thin and dispersive, which indicated that dispersion of clay nanoplatelets was achieved due to the clay modification with CTAB. According to the results of FTIR, XRD, SEM and TEM, it can be concluded that almost all CTAB intercalated into MMT interlayer with destroying the crystalline structure of MMT and then result in different influence on adsorption capacity of surfactant-modified MMT for CR, which will be discussed in the following sections in detail.

3.5. Effect of surfactants-modified MMT on adsorption

The effects of different kinds of surfactants-modified MMT on adsorption capacity of CR are shown in Fig. 6. It should be noted that each surfactant contains the amount of surfactant equivalent to 1.0 of the CEC of purified MMT. As can be seen from Fig. 6, it is note-

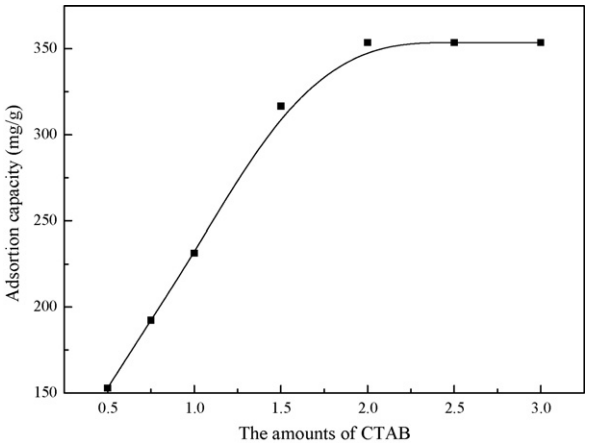

Fig. 7. Effect of the amounts of CTAB on adsorption capacity of CTAB-MMT for CR. Adsorption experiments—dye concentration, 800 mg/L; sample dose, 0.05 g/25 mL; natural pH 7.5; temperature, 30 °C; equilibrium time, 480 min.

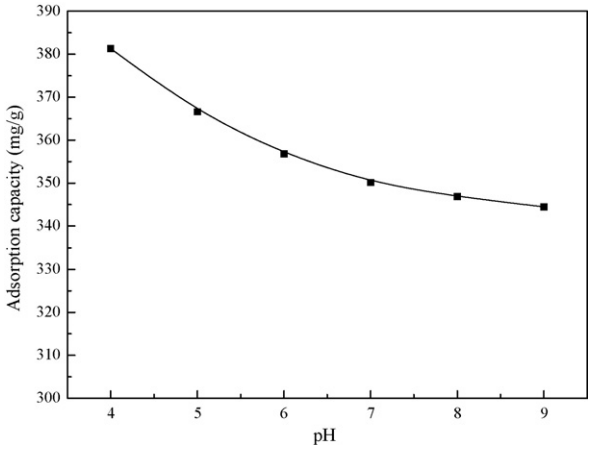

Fig. 8. Effect of the pH values on adsorption capacity of CTAB-MMT for CR. Adsorption experiments—dye concentration, 1000 mg/L; sample dose, 0.05 g/25 mL; pH range, 4.0–9.0; temperature, 30 °C; equilibrium time, 480 min.

worthy that the adsorption capacity of purified MMT (10.2 mg/g) for anion dye CR could be greatly improved when MMT was modified by surfactant. The adsorption capacity sharply increases from 31.1 to 229 mg/g with increasing the numbers of carbon atom of surfactant from 8 to 16 and then decreases with further increasing the numbers of carbon atom of surfactant from 16 to 18. The results may be due to the alkyl chain length of CTAB is suitable for intercalating into the MMT galleries, which in turn result in an increase in the absorption for CR. According to these results, CTAB is chosen as modifier for the surface modification of MMT in this study.

3.6. Effect of the amounts of CTAB on adsorption

Fig. 7 shows the effect of the amounts of CTAB on the adsorption capacities of CR onto CTAB-MMT. The adsorption capacities of CTAB-MMT increase with increasing of the amounts of CTAB. The observation can be explained that the amount of surfactant which intercalated into the MMT galleries increase with an increase of CTAB, which result in an increase in the absorption for CR. However, when the addition amount of CTAB exceeds 2.0 CEC of MMT, the adsorption capacities hardly increase which may be attributed to the amount of intercalated CTAB is saturated. Therefore, under our experimental conditions, CTAB-MMT with the amount of CTAB (2.0 CEC) possesses the highest adsorption capacity.

To further support the explanation mentioned above, we also investigated the effect of the amounts of CTAB on the specific surface area via BET nitrogen gas adsorption measurements and the average pore size of CTAB-MMT. The test results indicate, compared with purified MMT (61.4 m^2/g), the surface area of CTAB-MMT decrease with increasing of the amounts of CTAB. The specific surface areas of CTAB-MMT are 32.6, 18.6 and 8.10 m^2/g when the amounts of CTAB are equal to 0.5, 1.0 and 2.0 CEC of MMT, respectively. These are attributed to most of the exchange sites of CTAB-MMT satisfied by CTAB species with large molecular size and the inaccessibility of the internal surface to nitrogen gas [32]. However, the surfactants-modified MMT exhibit a larger average pore size than the precursor MMT. Compared with purified MMT (6.70 nm), the average pore size of CTAB-MMT increases from 9.30 to 13.6 nm with increasing of the amounts of CTAB from 0.5 to 1.0 CEC of MMT. The pore size of CTAB-MMT decrease from 13.6 to 11.5 nm with further increasing of the amounts of CTAB from 1.0 to 2.0 CEC of MMT. These results show that appropriate average pore size may be facilitate an increase of CR dye adsorption on CTAB-MMT and the synergic effects of these factors such as the changes in the crystalline structure (it also can be seen from Figs. 2–5), the specific surface area and the average pore size may be result in the higher adsorption capacity of the CTAB-MMT with the amount of CTAB (2.0 CEC) for CR dye. Therefore, the following discussion will be focused on the CTAB-MMT with the amount of CTAB (2.0 CEC) in this study.

3.7. Effect of pH value on adsorption

The effect of the pH value of the original solution on the adsorption capacity of CR dye is shown in Fig. 8. It can be seen that the effect of the pH on the adsorption capacity of CR dye is weak. When the pH value of the dye solution was raised from 4.0 to 9.0 (It should be noted that CR was slightly soluble in water at the pH 2), the adsorption capacity reduced slowly from 381 to 344 mg/g. The slight decrease in adsorption may be attributed to the repulsion between anionic dye molecules and the excessive hydroxyl ions at alkaline pH values. However, comparatively high adsorption capacity of the anionic dye on the adsorbent still occurred at pH 9.0 due to the fact that chemical interactions between CR dye and CTAB-MMT taken place. This can be further proved by the change in the FTIR spectra and SEM analysis of CTAB-MMT before and after dye adsorption (see Figs. 12 and 13).

3.8. Effect of temperature on adsorption

The effect of temperature on adsorption was studied at 30, 40 and 50 °C, and the results are shown in Table 2. As shown in Table 2, the amount of CR dye adsorption on CTAB-MMT increases with the increasing of temperature. The amount of dye adsorption increases from 350.13 to 399 mg/g when increasing initial solution temperature from 30 to 50 °C. It is found that higher temperature facilitated to the adsorption of CR on CTAB-MMT. It is well known that increasing temperature may produce a swelling effect within the internal structure of absorbent, penetrating the large dye molecule further

Table 2
Effect of the temperature on adsorption capacity of CTAB-MMT for CR

Temperature (°C)	Adsorption capacity (mg/g)
30	350
40	377
50	399

Adsorption experiments—dye concentration, 1000 mg/L; sample dose, 0.05 g/25 mL; pH 7.0; temperature, 30–50 °C; equilibrium time, 480 min.

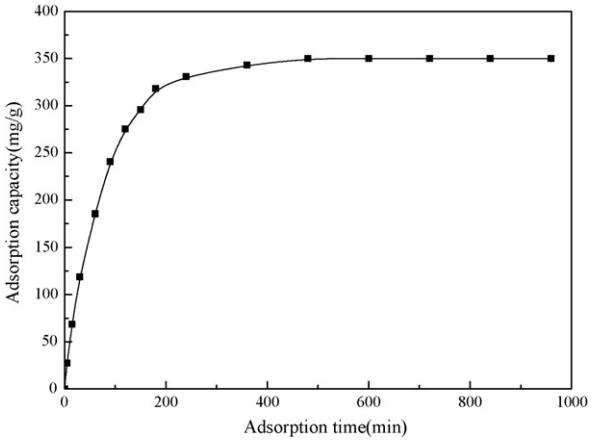

Fig. 9. Effect of the adsorption time on adsorption capacity of CTAB-MMT for CR. Adsorption experiments—dye concentration, 1000 mg/L; sample dose, 0.05 g/25 mL; pH 7.0; temperature, 30 °C.

[33]. A similar trend has been observed for the adsorption of CR on calcium-rich fly ash [15] and activated carbon prepared from coir pith [34].

3.9. Effect of adsorption time on adsorption

The effect of adsorption time on the adsorption capacities of CR is shown in Fig. 9. The adsorption capacity increased rapidly within 180 min and then slowly until the adsorption equilibrium was reached. Under our experimental conditions, the equilibrium time for the adsorption of CR on CTAB-MMT is 480 min.

3.10. Effect of the initial dye concentration on adsorption

Generally, the removal of dye was dependent on the initial concentration of the dye [13,34]. The relationship between the initial dye concentration and adsorption capacities of CR on CTAB-MMT is presented in Fig. 10. It can be seen that the adsorption capacities of CR increased sharply from 296 to 344 mg/g with increasing the initial dye concentration from 600 to 750 mg/L. However, the adsorption capacity for CR increased slightly from 344 to 350 mg/g with an increase in the initial concentration from 750 to 1100 mg/L. This result may be attributed to the fact that the aggregation of CR dye molecules makes it almost impossible for them to diffuse deeper into on CTAB-MMT structure [35,36].

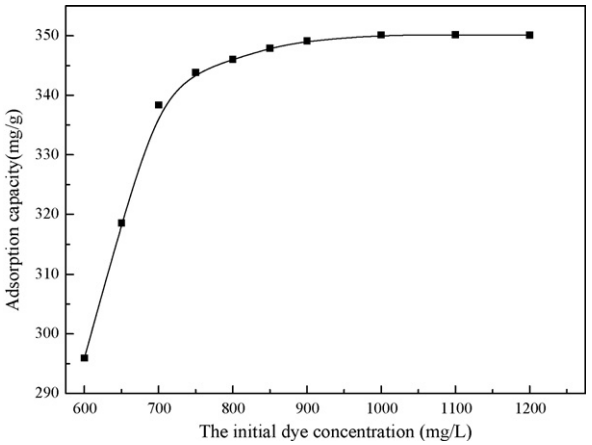

Fig. 10. Effect of the dye concentration on adsorption capacity of CTAB-MMT for CR. Adsorption experiments—sample dose, 0.05 g/25 mL; pH 7.0; temperature, 30 °C; equilibrium time, 480 min.

Table 3
The rate constants and the correlation coefficients of the two kinetic models

Pseudo-first-order model		Pseudo-second-order model	
k_1 ($\times 10^{-2}$ min^{-1})	R^2	k_2 ($\times 10^{-4}$ g/mg/min)	R^2
1.16	0.9612	5.05	0.9991

3.11. Adsorption kinetics

In order to investigate the adsorption processes of CR on the adsorbents, pseudo-first-order and pseudo-second-order models were used.

The pseudo-first-order equation [37] can be expressed as Eq. (2):

$$\log(q_e - q_t) = \frac{\log q_e - k_1 t}{2.303} \quad (2)$$

The pseudo-second-order model is based on the assumption of chemisorption of the adsorbate on the adsorbents [38]. This model [39] is given as Eq. (3):

$$\frac{t}{q_t} = \frac{1}{k_2 q_e^2} + \frac{t}{q_e} \quad (3)$$

where q_t is the amount of adsorption dye (mg/g) at time t (min) and k_1 (min^{-1}), k_2 (g/mg/min) are the adsorption rate constant of pseudo-first-order, pseudo-second-order adsorption, respectively. The validity of the two models can be interpreted by the linear plots of $\log(q_e - q_t)$ versus t and (t/q_t) versus t, respectively. The rate constants k_1 and k_2 can be obtained from the plot of experimental data.

The rate constants and the correlation coefficients of the two kinetic models are shown in Table 3. It is clearly seen that the pseudo-second-order kinetic model, compared with the pseudo-first-order model, describes the adsorption of CR on CTAB-MMT very well, which shows that the assumption of the chemisorptive nature of adsorbate–adsorbent system for the pseudo-second-order model is valid for CR–CTAB-MMT system investigated. These results also indicated that the adsorption rate of CR dye depends on the concentration of dye at the absorbent surface and the absorbance of these absorbed at equilibrium [40].

3.12. Adsorption isotherms

Fig. 11 shows the plot of adsorption isotherm, adsorption capacity versus the equilibrium dye concentration for the adsorption of CR on CTAB-MMT. It can be seen that at lower adsorbtion equi-

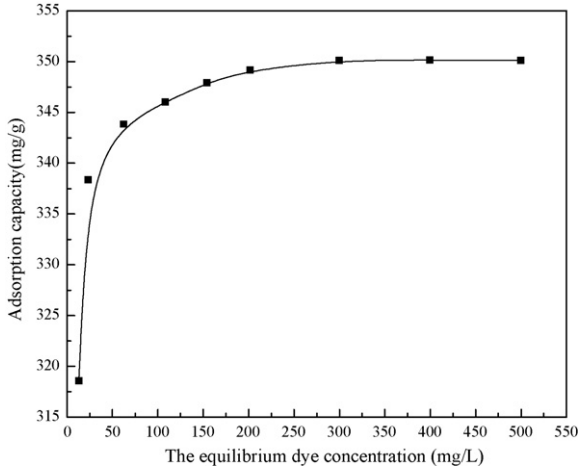

Fig. 11. The plot of adsorption isotherm for the adsorption of CR on CTAB-MMT. Adsorption experiments—sample dose, 0.05 g/25 mL; pH 7.0; temperature, 30 °C; equilibrium time, 480 min.

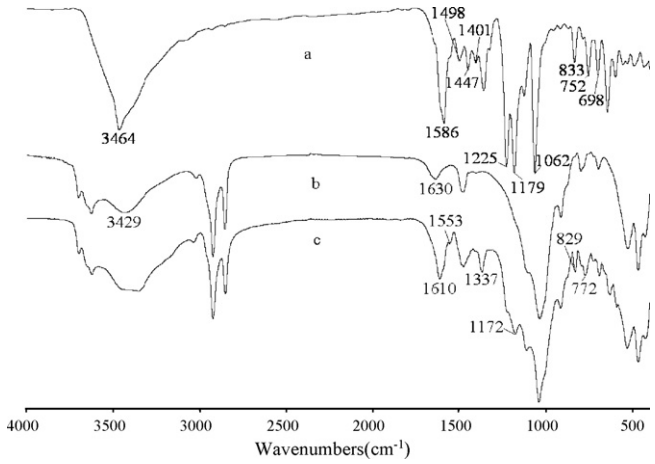

Fig. 12. IR spectra of CR (a), CTAB-MMT before (b) and after (c) dye adsorption.

librium dye concentration, adsorption capacity rises sharply and thereafter the increase is gradual with an increase of equilibrium dye concentration.

The equilibrium adsorption data were interpreted using Langmuir and Freundlich models [41], which are represented by the following equations, respectively:

$$\frac{C_e}{q_e} = \frac{1}{bq_m} + \frac{C_e}{q_m} \quad (4)$$

$$q_e = K_f C_e^{1/n} \quad (5)$$

where q_m (mg/g) and b (L/mg) are the Langmuir isotherm coefficients. The value of q_m represent the maximum adsorption capacity. K_f (mg/g) and n are the Freundlich constants. Two adsorption isotherms were constructed by plotting the C_e/q_e versus C_e, $\lg q_e$ versus $\lg C_e$, respectively.

The values of R^2 of Langmuir and Freundlich models are 0.9999 and 0.8652, respectively. In addition, the q_m value for the adsorption of CR by CTAB-MMT was 351 mg/g, which are same as the experiment data 350 mg/g for CTAB-MMT. It can be seen that the adsorption of CR is in good agreement with the Langmuir isotherm rather than the Freundlich isotherm. This indicates the surface of CTAB-MMT was covered by the monolayer of CR molecules. Similar behavior was also found for the adsorption of CR onto red mud [14], activated coir pith [34] and mesoporous activated carbons [42]. The q_m values for the adsorption of CR by waste Fe(III)/Cr(III) hydroxide, waste orange peel, waste banana pith, biogas waste slurry, waste red mud and paddy straw were 44.00 mg/g [12], 22.44 mg/g [13], 20.29 mg/g [10], 9.50 mg/g [9], 4.05 mg/g [14], 1.01 mg/g [11], respectively. The higher q_m value of 52–189 mg/g was achieved using mesoporous activated carbons [42]. However, these values are considerably lower compared to the q_m (351 mg/g) determined for the CR adsorption onto CTAB-MMT. So it can be effectively used as an adsorbent in treatment of CR dye wastewaters.

3.13. Adsorption mechanism of CR dye

3.13.1. FTIR spectra

FTIR spectra of CR (a) and CTAB-MMT before (b) and after (c) the adsorption are presented in Fig. 12. The major differences are: the absorption band at 3464 cm^{-1} (Fig. 12a), corresponding to the stretching vibration of –N–H in the structure of dye CR, diminishes after adsorption with CTAB-MMT (Fig. 12c). The band at 1586 cm^{-1}, assigned to –N=N– stretching (Fig. 12a), diminishes after adsorption (Fig. 12c). At the same time, the strong bands at 1225, 1179, and 1062 cm^{-1}, attributed to S=O stretching (Fig. 12a), also diminish after adsorption (Fig. 12c). The results indicated that the NH_2, –N=N– and $–SO_3$ groups of CR were involved in the adsorption process. Furthermore, the bands at 1498, 1447, 1402 cm^{-1}, attributed to aromatic skeletal vibrations, have been shifted, broadened, and reduced after adsorption. The bands at 833, 752, 698 cm^{-1}, assigned to characteristic adsorption of aromatic skeletal groups have been also reduced after adsorption. Moreover, the IR spectra of CTAB-MMT before and after dye adsorption indicated that the wide absorption band at 3429 cm^{-1} (Fig. 12b), corresponding to –OH stretching vibration of H_2O of MMT, broadened and strengthened after adsorption (Fig. 12c). The absorption bands at 1630 cm^{-1} (Fig. 12b), assigned to the absorption band of –OH stretching vibration of H_2O of MMT, strengthened and shift to lower wave number 1610 cm^{-1} (Fig. 12c). Compared with the IR spectra of CTAB-MMT before dye adsorption (Fig. 12b), the new absorption bands (1553, 1337, 1172, 829, 772 cm^{-1}) were observed on CTAB-MMT after dye adsorption. The IR analysis results suggest that CR on CTAB-MMT is held by chemical activation or chemisorption, probably indicating CTAB-MMT/dye complexation.

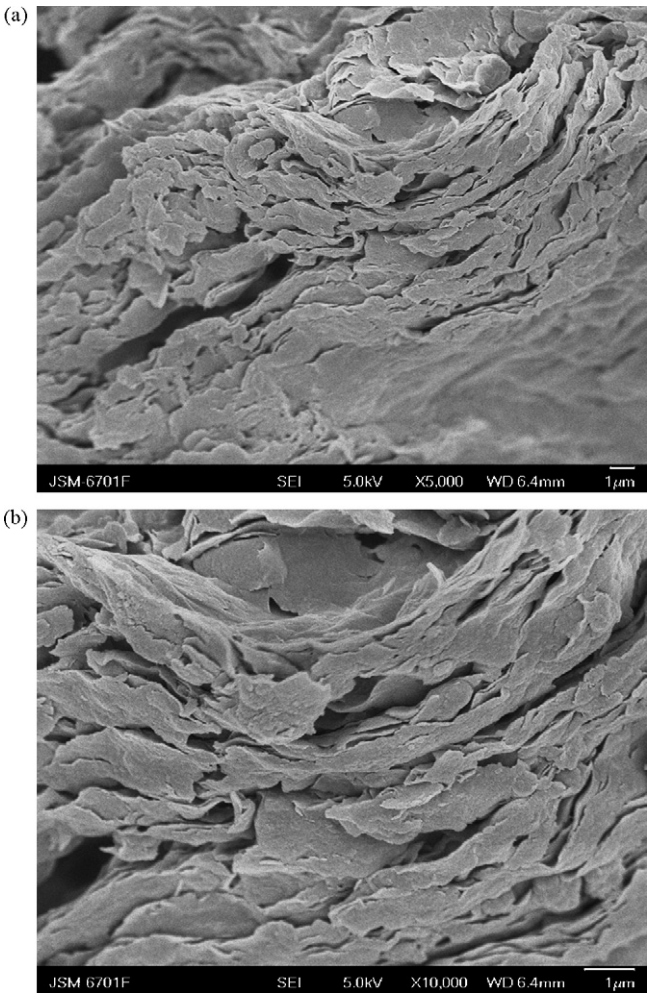

Fig. 13. SEM images of CTAB-MMT before (a) and after (b) the adsorption.

3.13.2. SEM analysis

The SEM images of CTAB-MMT before and after the adsorption are shown in Figs. 4d and 13 ($a \times 5000$, $b \times 10{,}000$), respectively. CTAB-MMT after the adsorption displays lamellar curly surface compared with the coarse porous surface of CTAB-MMT before the adsorption. These results indicate that the adsorption of CTAB-

MMT for CR may be a chemical interaction between CTAB-MMT and dye CR, which again substantiate the mechanism of adsorption mentioned in above studies.

4. Conclusion

Surfactant-modified MMT were synthesized with OTAB, DTAB, CTAB and STAB. Compared with purified MMT (10.2 mg/g), the adsorption capacities of surfactant-modified MMT samples for CR (31.1, 83.6, 229 and 127 mg/g for OTAB-MMT, DTAB-MMT, CTAB-MMT and STAB-MMT, respectively) were greatly improved and CTAB-MMT exhibited the higher adsorption capacities for CR. The synergic effects of the factors such as the changes in the crystalline structure, the specific surface area and the average pore size may be result in the higher adsorption capacity of the CTAB-MMT with the amount of CTAB (2.0 CEC) for CR dye.

In this investigation, the effects of amounts of CTAB, initial pH value of the dye solution, adsorption temperature, adsorption time and the initial dye concentration were investigated. The results indicated that the adsorption capacity of CTAB-MMT for CR decreased with increasing pH but increased with increasing temperature. The adsorption process of the CR dye on CTAB-MMT followed the pseudo-second-order and the Langmuir isotherm, respectively. The Langmuir adsorption capacity was 351 mg/g. The IR analysis and SEM analysis results suggested that the adsorption of CTAB-MMT for CR was a chemical adsorption process between CTAB-MMT and the NH_2, –N=N– and $–SO_3$ groups of CR. This study showed that the CTAB-MMT is useful as a promising adsorbent for the remove of CR dye in wastewater treatment.

Acknowledgement

This work was financially supported with the science and technology major project of Jiangsu Province (No. BS2007118).

References

[1] R. Sivraj, C. Namasivayam, K. Kadirvelu, Orange peel as an adsorbent in the removal of acid violet 17(acid dye) from aqueous solution, Waste Manage. 21 (1) (2001) 105–110.
[2] G. McKay, M.S. Otterburn, D.A. Aga, Fullers earth and fired clay as adsorbent for dye stuffs. Equilibrium and rate constants, Water Air Soil Pollut. 24 (1985) 307–322.
[3] P.K. Dutta, An overview of textile pollution and itsremedy, Indian J. Environ. Prot. 14 (6) (1994) 443–446.
[4] A.R. Gregory, J. Elliott, P. Kluge, Ames testing of direct black 38 parallels carcinogenicity testing, J. Appl. Toxicol. 1 (6) (1981) 308–313.
[5] M. Neamtu, A. Yediler, I. Siminiceanu, M. Macoveanu, A. Kellrup, Decolorization of disperse red 354 azo dye in water by several oxidation processes—a comparative study, Dyes Pigments 60 (1) (2004) 61–68.
[6] P.K. Malik, S.K. Sanyal, Kinetics of decolourisation of azo dyes in wastewater by UV/H_2O_2 process, Sep. Purif. Technol. 36 (3) (2004) 167–175.
[7] S. Chakraborty, M.K. Purkait, S. DasGupta, S. De, J.K. Basu, Nanofiltration of textile plant effluent for color removal and reduction in COD, Sep. Purif. Technol. 31 (2) (2003) 141–151.
[8] S.J. Allen, Types of Adsorbent Materials—Use of Adsorbents for the Removal of Pollutants from Wastewaters, CRC, Boca Raton, FL, USA, 1996, p. 59.
[9] C. Namasivayam, R.T. Yamuna, Removal of Congo Red from aqueous solutions by biogas waste slurry, J. Chem. Technol. Biotechnol. 53 (22) (1992) 153–157.
[10] C. Namasivayam, N. Kanchana, Waste banana pith as adsorbent for colour removal from wastewaters, Chemosphere 25 (11) (1992) 1691–1705.
[11] N. Deo, M. Ali, Dye adsorption by a new low cost material: Congo Red—1, Indian J. Environ. Prot. 13 (7) (1993) 496–508.
[12] C. Namasivayam, R. Jeyakumar, R.T. Yamuna, Dye removal from wastewater by adsorption on waste Fe(III)/Cr(III) hydroxide, Waste Manage. 14 (7) (1994) 643–648.
[13] C. Namasivayam, N. Muniasamy, K. Gayathri, M. Rani, K. Ranganathan, Removal of dyes from aqueous solutions by cellulosic waste orange peel, Bioresour. Technol. 57 (1) (1996) 37–43.
[14] C. Namasivayam, D.J.S.E. Arasi, Removal of Congo Red from wastewater by adsorption onto waste red mud, Chemosphere 34 (2) (1997) 401–417.
[15] B. Acemioğlu, Adsorption of Congo Red from aqueous solution onto calcium-rich fly ash, J. Colloid Interface Sci. 274 (2) (2004) 371–379.
[16] G. McKay, Adsorption of dyestuffs from aqueous solutions with activated carbon. I. Equilibrium and batch contact-time studies, J. Chem. Technol. Biotechnol. 32 (7) (1982) 759–772.
[17] R.A. Shawabkeh, M.F. Tutunji, Experimental study and modeling of basic dye sorption by diatomaceous clay, Appl. Clay Sci. 24 (1–2) (2003) 111–120.
[18] M.G. Neumann, F. Gessner, C.C. Schmitt, R. Sartori, Influence of the layer charge and clay particle size on the interactions between the cationic dye methylene blue and clays in an aqueous suspension, J. Colloid Interface Sci. 255 (2) (2002) 254–259.
[19] A.H. Gemeay, A.S. El-Sherbiny, A.B. Zaki, Adsorption and kinetic studies of the intercalation of some organic compounds onto Na^+-montmorillonite, J. Colloid Interface Sci. 245 (1) (2002) 116–125.
[20] N. Miyamoto, R. Kawai, K. Kuroda, M. Ogawa, Adsorption and aggregation of a cationic cyanime dye on layered clay minerals, Appl. Clay Sci. 16 (3–4) (2000) 161–170.
[21] A.H. Gemeay, Adsorption characteristics and the kinetics of cation exchange of rhodamine 6G with Na^+-montmorillonite, J. Colloid Interface Sci. 251 (2) (2002) 235–241.
[22] T.A. Wolfe, T. Demirel, E.R. Baumann, Interaction of aliphatic amines with montmorillonite to enhance adsorption of organic pollutants, Clays Clay Miner. 33 (4) (1985) 301–307.
[23] E. Klumpp, H. Heitmann, M.J. Schwuger, Synergetic effects between cationic surfactants and organic pollutants on clay minerals, Colloids Surf. A: Physicochem. Eng. Aspects 78 (1993) 93–98.
[24] E. Klumpp, M.J. Schwuger, Detergents in the Environment, Marcel Dekker, New York, 1997.
[25] J.A. Smith, A. Galan, Sorption of nonionic organic contaminants to single and dual organic cation bentonites from water, Environ. Sci. Technol. 29 (3) (1995) 685–692.
[26] E. Klumpp, C. Contreras-Ortega, P. Klahre, F.J. Tino, S. Yapar, C. Portillo, S. Stegen, F. Queirolo, M.J. Schwuger, Sorption of 2,4-dichlorophenol on modified hydrotalcites, Colloids Surf. A: Physicochem. Eng. Aspects 230 (1–3) (2003) 111–116.
[27] L. Capovilla, P. Labbe, G. Reverdy, Formation of cationic/anionic mixed surfactant bilayers on laponite clay suspensions, Langmuir 7 (10) (1991) 2000–2003.
[28] M.M. Mortland, S. Shaobai, S.S. Boyd, Clay–organic complexes as adsorbents for phenol and chlorophenols, Clays Clay Miner. 34 (1986) 581–585.
[29] S.A. Boyd, M.M. Mortland, C.T. Chiou, Sorption characteristic of organic compounds on hexadecyltrimethylammonium-smectite, Soil Sci. Soc. Am. J. 52 (1988) 652–657.
[30] S.A. Boyd, S. Shaobai, J.F. Lee, M.M. Mortland, Pentachlorophenol sorption by organo-clays, Clays Clay Miner. 36 (2) (1988) 125–130.
[31] S. Xu, G. Sheng, S.A. Boyd, Use of organoclays in pollution abatement, Adv. Agron. 59 (1997) 25–62.
[32] C.C. Wang, L.C. Juang, T.C. Hsu, C.K. Lee, J.F. Lee, F.C. Huang, Adsorption of basic dyes onto montmorillonite, J. Colloid Interface Sci. 273 (1) (2004) 80–86.
[33] K.G. Bhattacharyya, A. Sarma, Adsorption characteristics of the dye, brilliant green, on neem leaf powder, Dyes Pigments 57 (3) (2003) 211–222.
[34] C. Namasivayam, D. Kavitha, Removal of Congo Red from water by adsorption onto activated carbon prepared from coir pith, an agricultural solid waste, Dyes Pigments 54 (1) (2002) 47–58.
[35] I.D. Mall, V.C. Srivastava, N.K. Agarwal, I.M. Mishra, Removal of Congo Red from aqueous solution by bagasse fly ash and activated carbon: kinetic study and equilibrium isotherm analyses, Chemosphere 61 (4) (2005) 492–501.
[36] I.D. Mall, V.C. Srivastava, G.V.A. Kumar, I.M. Mishra, Characterization and utilization of mesoporous fertilizer plant waste carbon for adsorptive removal of dyes from aqueous solution, Colloids Surf. A: Physicochem. Eng. Aspects 278 (1–3) (2006) 175–187.
[37] S. Lagergren, About the theory of so-called adsorption of soluble substances, Kungliga Svenska Vetenskapsakademiens, Handlingar 24 (4) (1898) 1–39.
[38] V.C. Srivastava, I.D. Mall, I.M. Mishra, Adsorption of toxic metal ions onto activated carbon study of sorption behaviour through characterization and kinetics, Chem. Eng. Process., in press.
[39] Y.S. Ho, G. McKay, Pseudo-second order model for sorption processes, Process Biochem. 34 (5) (1999) 451–465.
[40] S.L. Sun, A.Q. Wang, Adsorption kinetics of Cu(II) ions using *N*,*O*-carboxymethyl-chitosan, J. Hazard. Mater. 131 (1–3) (2006) 103–111.
[41] K. Periasamy, C. Namasivayam, Removal of nickel(II) from aqueous solution and nickel plating industry wastewater industry using an agriculture waste: peanut hull, Waste Manage. 15 (1) (1995) 63–68.
[42] E.L. Grabowska, G. Gryglewicz, Adsorption characteristics of Congo Red on coal-based mesoporous activated carbon, Dyes Pigments 74 (1) (2006) 34–40.